TURBULENCE, STRING THEORY AND ISING MODEL

A PREPRINT

Alexander Migdal
Department of Physics, New York University
726 Broadway, New York NY 10003

December 21, 2024

ABSTRACT

We advance the vortex cell approach to turbulence [1] by elaborating the Clebsch field dynamics on the surface of vortex cells. We argue that resulting statistical system can be described as 3D Ising model interacting with Compactified Bosonic String on the Riemann surface describing phase boundary. The cells come out as $\sigma = 1$ phase of the Ising model in strong magnetic field. At large circulation around large loop the dominant Ising configuration correspond to minimal volume cells covering the area inside the loop, which naturally leads to the Area law.

1 Introduction

In the recent papers [2, 3, 4, 5] we revived and advanced the old conjecture [6] that tails of velocity circulation PDF in inertial range of developed turbulence are determined by a minimal surface bounded by a given loop. This conjecture was (to some extent) confirmed in recent numerical experiments [7], which inspired this renewed interest to the Loop Equations of [6].

The basic variable in the Loop Equations a circulation around closed loop in coordinate space

$$\Gamma[C] = \oint_C \vec{v} d\vec{r} \tag{1}$$

The PDF for velocity circulation as a functional of the loop

$$P\left(C,\Gamma\right) = \langle \delta\left(\Gamma - \Gamma[C]\right)\rangle \tag{2}$$

with brackets <> corresponding to time average or average over random forces, was shown to satisfy certain functional equation (loop equation).

The PDF for Γ is much simpler than that of the usual velocity field, partly because the long-range fluctuations of the time derivative of velocity field creating the complexity of multi-fractal scaling laws come from the longitudinal ∇h components of $\dot{v}$ in momentum space, which drop in the circulation because of its gauge invariance $\vec{v} \Rightarrow \vec{v} + \nabla\phi$.

The original conjecture of [6], based on asymptotic form of the Loop Equation was that

$$P\left(C,\Gamma\right) \sim \exp\left(-b|\Gamma|^{\mu} A_C^{-\mu\alpha}\right) \tag{3}$$

where μ, α were some universal indices, and A_C was the area of the minimal surface. This form of the PDF was recently confirmed in numerical experiments of [7] with $\mu \approx 0.82, \alpha \approx 0.55$. The exponential law was confirmed over 8 orders of magnitude and its universality was verified.

In recent papers we analyzed the loop equation in some detail and found that the Area solution has to be modified to apply to arbitrary non-planar loops:

$$A_C = \int_{S_C} d\sigma(r)\Phi(r) \tag{4}$$

where S_C is minimal surface bounded by C with area element $d\sigma(r)$ and $\Phi(r)$ is some 2-dimensional scalar field on the surface (we call it Φ here to avoid confusion with 3-D vorticity field $\Omega_\alpha(r)$ below). We derived integral equation [5] for this $\Phi(r)$ and found some analytic as well as numerical solutions. The critical index $\alpha = \frac{1}{2}$ was predicted [4] from the loop equations. The experimental value 0.55 is closer to this prediction than to the Kolmogorov value $\frac{2}{3}$. Moreover, the apparent difference $\alpha - 0.5 = 0.05$ can be explained as a sub-leading term in the scaling index $\lambda(p) \to 2p\alpha$ of momenta $\langle \Gamma[C]^p \rangle \propto A_C^{0.5\lambda(p)}$ (see [4]).

The numerical simulation still have not answered crucial question of spatial distribution of vorticity responsible for the circulation statistics. The modified Area law (4) does not necessarily mean homogeneous distribution of $\Phi(r)$ along the minimal surface, so it can be concentrated at the edge, i.e. the loop itself.

In this paper we revive the Liouville Equation approach to Turbulence in [1] to provide some new insight on the geometric structures behind the circulation statistics. We are led to amazing equivalence of Turbulence to 3D Ising model interacting with S^1 Compactified Bosonic String on the phase boundaries.

2 Liouville Equation and Vortex Cell Dynamics

As it was discussed in detail in my old work [1] the equilibrium distribution P of isotropic turbulence has to depend on the conserved quantity, i.e. the one commuting with Hamiltonian

$$H = \int d^3 r \frac{v_\alpha(r)^2}{2} \tag{5}$$

in a sense of Poisson brackets.

$$\partial_t P = [H, P] = 0 \tag{6}$$

In this section we repeat the basic results of that old work in a hope that this time around, with more elaborate discussion and some typos fixed it will be easier to understand. Besides, now we derive some observable consequences of that vortex cell dynamics, so this is more than mathematical exercise.

We shall use Greek letters for spatial indices of vectors in Euler frame (i.e. static against flow) and Latin letters for indices of vectors moving with the flow. In particular the coordinates $X_\alpha(\rho)$ map initial conditions ρ_a to the moving point $r_\alpha = X_\alpha(\rho)$ in the flow.

The Euler equations can be written in manifestly Hamiltonian form

$$\partial_t v_\alpha = \int d^3 r' T_{\alpha\nu}(r - r') v_\mu(r') \omega_{\mu\nu}(r') = [H, v_\alpha] \tag{7}$$

where $\omega_{\alpha\beta} = \partial_\alpha v_\beta - \partial_\beta v_\alpha$ is vorticity tensor and

$$T_{\alpha\beta}(r) = \delta_{\alpha\beta}\delta(r) + \partial_\alpha \partial_\beta \frac{1}{4\pi |r|} \tag{8}$$

is the projection operator for incompressibility condition

$$\partial_\alpha v_\alpha(r) = 0 \tag{9}$$

The Poisson brackets of velocity components

$$[v_\alpha(r_1), v_\beta(r_2)] = \int d^3 r T_{\alpha\mu}(r_1 - r) T_{\beta\nu}(r_2 - r) \omega_{\mu\nu}(r) \tag{10}$$

The Liouville theorem of phase space volume conservation follows from this Hamiltonian dynamics

$$\frac{\delta}{\delta v_a(r)} [H, v_a] = 0 \tag{11}$$

$$(Dv) = \prod_r d^3 v(r) = \text{const} \tag{12}$$

The Gibbs distribution $P = \exp(-\beta H)$ manifestly commutes with the Hamiltonian, but it is not appropriate in turbulence problem for variety of reasons, starting with the fact that Hamiltonian integral density diverges at large scales (or at small wavelengths in Fourier space) because of infrared divergences $\int dk k^{-5/3}$.

In order to find a substitute for the Gibbs distribution we study dynamics of the Lagrange coordinates of the flow.

The field $X_\alpha(\rho)$ moves with the flow (the Helmholtz equation)

$$\partial_t X_\alpha(\rho) = v_\alpha(X(\rho)) \tag{13}$$

The contribution of all cells D to the net velocity field can be written as sum of Biot-Savart integrals

$$v_\alpha(r) = -e_{\alpha\beta\gamma}\partial_\beta \sum_i \int_{D_i} d^3\rho \frac{\Omega_\gamma(\rho)}{4\pi|r - X(\rho)|} \tag{14}$$

where

$$\Omega_\gamma(\rho) = \Omega^a(\rho)\partial_a X_\gamma(\rho) \tag{15}$$

is the vorticity vector in the Euler frame. The vorticity vector $\Omega^a(\rho)$ in the Lagrange frame is conserved

$$\partial_t \Omega^a(\rho) = 0 \tag{16}$$

The physical vorticity tensor $\omega_{\alpha\beta} = \partial_\alpha v_\beta - \partial_\beta v_\alpha$ inside the cell can be readily computed from velocity integral. The gradients produce the δ function so that we get

$$\omega_{\alpha\beta}(X(\rho)) = \left(\frac{\partial(X_1, X_2, X_3)}{\partial(\rho_1, \rho_2, \rho_3)}\right)^{-1} e_{\alpha\beta\gamma}\Omega_\gamma(\rho) \tag{17}$$

or in Euler frame, inverting $\rho = X^{-1}(r)$

$$\omega_{\alpha\beta}(r) = \frac{1}{6}\, e_{\lambda\mu\nu}\, e_{abc}\partial_\lambda\rho^a\partial_\mu\rho^b\partial_\nu\rho^c\, e_{\alpha\beta\gamma}\, \Omega^f(\rho)\partial_f X_\gamma = e_{abc}\partial_\alpha\rho^a(r)\partial_\beta\rho^b(r)\,\Omega^c(\rho(r)) \tag{18}$$

The inverse matrix $\partial_\alpha\rho^a = (\partial_a X_\alpha)^{-1}$ relates the Euler indexes to the Lagrange ones, as it should. These relations between the Euler and Lagrange vorticity are equivalent to the conservation of the vorticity 2-form

$$\Omega = \sum_{\alpha<\beta} \omega_{\alpha\beta}(X) dX_\alpha \wedge dX_\beta = \sum_{a<b} \Omega_{ab}(\rho) d\rho^a \wedge d\rho^b;\ \Omega_{ab} = e_{abc}\Omega^c \tag{19}$$

which is the Kelvin theorem of the conservation of velocity circulation around arbitrary fluid loop.

In Appendix B of [1] we derive the Euler equation from the Helmholtz equation and study the general properties of the former. We show that this is equivalent to the Hamiltonian dynamics with the (degenerate) Poisson brackets

$$[X_\alpha(\rho), X_\beta(\rho')] = -\delta^3(\rho - \rho')e_{\alpha\beta\gamma}\frac{\Omega_\gamma(\rho)}{\Omega^2_\mu(\rho)} \tag{20}$$

The Hamiltonian is given by the same fluid energy, with the velocity understood as functional of $X(.)$ The degeneracy of the Poisson brackets reflects the fact that there are only two independent degrees of freedom at each point. This leads to the gauge symmetry which we discuss below.

The Hamiltonian variation reads

$$\frac{\delta H}{\delta X_\alpha(\rho)} = e_{\alpha\beta\gamma} v_\beta\left(X(\rho)\right)\Omega_\gamma(\rho) \tag{21}$$

This variation is orthogonal to velocity, which provides the energy conservation. It is also orthogonal to vorticity vector which leads to the gauge invariance. The gauge transformations

$$\delta X_\alpha(\rho) = f(\rho)\Omega_\alpha(\rho) \tag{22}$$

leave the Hamiltonian invariant. These transformations reparametrize the coordinates

$$\delta\rho^a = f(\rho)\Omega^a(\rho) \tag{23}$$

The vorticity density transforms as follows

$$\delta\Omega^a = -\Omega^a\partial_b(f\Omega^b) + f\Omega^b\partial_b\Omega^a + \Omega^b\partial_b(f\Omega^a) = 2f\Omega^b\partial_b\Omega^a \tag{24}$$

The first term comes from the volume transformation, the second one - from the argument transformation and the third one - from the vector index transformation of Ω so that

$$d^3\rho\,\Omega^a\partial_a = \text{inv} \tag{25}$$

The identity

$$\partial_a \Omega^a = 0 \tag{26}$$

was taken into account. We observe that these gauge transformations leave invariant the whole velocity field, not just the Hamiltonian.

This gauge invariance is less than the full diffeomorphism group which involves arbitrary function for each component of ρ. However, the Biot-Savart formula is also invariant with respect to full diffeomorphism group. One can rewrite it in manifestly invariant form [1]

$$v_\alpha(r) = -e_{\alpha\beta\gamma}\partial_\beta \sum_i \int_{D_i} \frac{dX_\gamma \wedge \Omega}{4\pi|r - X(\rho)|}. \tag{27}$$

Helmholtz equation is also manifestly parametric invariant [1].

The equations of motion, which literally follow from above Poisson brackets describe the motion in the direction orthogonal to the gauge transformations, namely

$$\partial_t X_\alpha(\rho) = \left(\delta_{\alpha\beta} - \frac{\Omega_\alpha(\rho)\Omega_\beta(\rho)}{\Omega_\mu^2(\rho)}\right) v_\beta\left(X(\rho)\right) = v_\alpha(X(\rho)) + f(\rho)\Omega_\alpha(\rho) \tag{28}$$

The difference is unobservable, due to gauge invariance. We could have defined the Helmholtz equation this way from the very beginning. The conventional Helmholtz dynamics represents so called generalized Hamiltonian dynamics, which cannot be described in terms of the Poisson brackets. The formula (21) cannot be solved for the velocity field because the matrix

$$\Omega_{\alpha\beta}(\rho) = e_{\alpha\beta\gamma}\Omega_\gamma(\rho) \tag{29}$$

cannot be inverted (there is the zero mode $\Omega_\beta(\rho)$). The physical meaning is the gauge invariance which allows us to perform the gauge transformations in addition to the Lagrange motion of the fluid element.

Formally, the inversion of the $\Omega-$matrix can be performed in a subspace which is orthogonal to the zero mode. The inverse matrix $\Omega^{\beta\gamma}$ in this subspace satisfies the equation

$$\Omega_{\alpha\beta}\Omega^{\beta\gamma} = \delta_{\alpha\gamma} - \frac{\Omega_\alpha\Omega_\gamma}{\Omega_\mu^2} \tag{30}$$

which has the unique solution

$$\Omega^{\beta\gamma} = -e_{\alpha\beta\gamma}\frac{\Omega_\alpha}{\Omega_\mu^2} \tag{31}$$

This solution leads to our Poisson brackets.

The vorticity 2-form simplifies in the Clebsch variables

$$\Omega^a = e^{abc}\partial_b\phi_1(\rho)\partial_c\phi_2(\rho) \tag{32}$$

$$\Omega = d\phi_1 \wedge d\phi_2 = \text{inv} \tag{33}$$

The Clebsch variables provide the bridge between the Lagrange and the Euler dynamics. By construction they are conserved, as they parametrize the conserved vorticity. The Euler Clebsch fields $\Phi_i(r)$ can be introduced by solving the equation $r = X(\rho)$

$$\Phi_i(r) = \phi_i\left(X^{-1}(r)\right) \tag{34}$$

These Euler Clebsch fields were studied by Yakhot and Zakharov [8] where the conservation law of Clebsch "particles" was observed and some estimates of Kolmogorov cascade leading to his famous $5/3$ law were presented. The difference between that work and our independent work in [1] was that we were introducing Clebsch field only inside cells, rather than in whole space. This will be discussed in more detail below.

Unlike the vorticity field, the Clebsch variables cannot be defined globally in the whole space. The inverse map $\rho = X^{-1}(r)$ is defined separately for each cell, therefore one cannot write $v_\alpha = \Phi_1\partial_\alpha\Phi_2 + \partial_\alpha\Phi_3$ everywhere in space. Rather one should add the contributions from all cells to the Biot-Savart integral, as we did before.

The most important for us consequence of this generalized Hamiltonian dynamics for $X_\alpha(\rho)$ is the conservation of the volume element

$$J(X,\rho) = \frac{\partial\left(X_1, X_2, X_3\right)}{\partial\left(\rho_1, \rho_2, \rho_3\right)} \tag{35}$$

[1] I am grateful to S. Dubovsky, who pointed to my omission of the full diffeopmorphism invariance of the Euler flow.

$$\partial_t J(X,\rho) = J(X,\rho)\partial_\alpha v_\alpha(X) = 0 \tag{36}$$

This means that the volume of each vortex cell is conserved in dynamics

$$V_i = \int_{D_i} d^3\rho J(X,\rho) = \text{inv}; \tag{37}$$

The volume is parametric invariant and can be written as an integral of 3-form

$$V_i = \int_{D_i} dX \wedge dX \wedge dX = \int_{D_i} d^3\rho e_{\mu\nu\lambda}\partial_1 X_\mu \partial_2 X_\nu \partial_3 X_\lambda \tag{38}$$

Parametric invariance comes about because the transformation of Jacobian $J(X,\rho)$ cancels with transformation of the volume element.

Note that the induced metric in 3D space

$$G_{ab} = \partial_a X_\mu \partial_b X_\mu \tag{39}$$

while being parametric covariant, is not conserved in Helmholtz dynamics unlike the volume element $J(X,\rho)$. So we cannot build 3D invariant functionals other than the volume of the cell.

However, the boundary invariants exist as we shall see now. In fact this volume is so-called Wess-Zumino term in string theory

$$V_i = \int_{D_i} dX \wedge dX \wedge dX = \int_{\partial D_i} dX \wedge dX \wedge X \tag{40}$$

which in fact only depends of the boundary values of the X field.

Let us introduce parametric equation corresponding to the bounbdary of the cell in ρ space

$$\partial D : \rho_a = Y_a(\xi) \tag{41}$$

$$\xi = \{u, v\} \tag{42}$$

with induced metric on the boundary:

$$g_{ij} = \partial_i Y_a \partial_j Y_a \tag{43}$$

This equation of the boundary $Y_a(\xi)$ of each cell is a motion invariant, unlike the physical coordinates $X_\mu(\rho \in \partial D) = X(Y_a(.))$.

Now we can define the internal area

$$S_i = \int_{\partial D_i} d^2\xi\sqrt{g} \tag{44}$$

which is another conserved quantity. In fact, the volume is a functional of the boundary values of $X^B(\xi) = X(Y(\xi))$:

$$V_i = \int_{\partial D_i} d^2\xi e_{\mu\nu\lambda}\partial_1 X^B_\mu(\xi)\partial_2 X^B_\nu(\xi) X^B_\lambda(\xi) \tag{45}$$

These net volume and net area, being motion and parametric invariant could serve in place of Hamiltonian in the Gibbs distribution

$$P = \exp\left(-\beta\sum_i V_i - \gamma\sum_i S_i\right) \tag{46}$$

These vortex cells look like an ideal gas but there is an implicit interaction via excluded volume. As it is argued in [1] the cells cannot intersect nor self-intersect as this would be a singularity in inverse function $\rho(X)$. Such cells are described by self-avoiding surfaces enclosing them.

In addition to the shapes and locations of vorticity drops there is of course the vorticity inside cells, parametrized by Clebsch variables. As we observed in old work [1] (see also below), there are no parametric invariant volume integrals of vorticity in three dimensions. However, we can construct surface invariants using induced metric.

The lowest order local effective Lagrangian for these variables compatible with parametric invariance, translation invariance $\phi_i \Rightarrow \phi_i + a_i$ and $U(1)$ symmetry of phase transformation of complex field $\psi = \phi_1 + \imath\,\phi_2$ is Clebsch Hamiltonian

$$H_C = \frac{1}{4\pi}\sum_D \int_{\partial D} d^2\xi\sqrt{g}g^{ij}\partial_i\bar{\psi}\partial_j\psi \tag{47}$$

Note that we did not add any potential term for the Clebsch field, as it would violate above-mentioned translation invariance. Normalization of the Clebsch Hamiltonian is a matter of convention.

3 Clebsch Boundary Conditions and String Compactification

There are some important boundary conditions for the Clebsch field, restricting the number of free variables. The fact that vorticity is zero outside the cell, means that there should be no flux outside. The normal direction given by

$$n_a \propto e_{abc}\partial_1 Y_a(\xi)\partial_2 Y_b(\xi) \tag{48}$$

The zero flux condition thus reads

$$\left[n_a e_{abc}\partial_b\bar{\psi}\partial_c\psi\right]_{\partial D} = 0 \tag{49}$$

or equivalently

$$\oint_{\delta C\in\partial D}\bar{\psi}d\psi = 0 \tag{50}$$

for every infinitesimal loop δC at the boundary ∂D of the cell. This can be achieved with the complex field ψ taking values on a circle $|\psi| = R$ at the boundary of the cell (see below).

So, the vorticity does not flow outside cells, it is confined inside, pretty much like gluon field is confined to the world sheet of the flux tube connecting quarks. This analogy inspired my conjectures about minimal surface in Turbulence. Now we can move this analogy one step further.

As vorticity is parametrized by Clebsch field which is defined only inside cells, what we have in this theory can be called Clebsch confinement and Clebsch field plays the role of "quarks of turbulence". The charge of this field corresponds to unbroken $U(1)$ symmetry and all observables are neutral with respect to this charge. Moreover,as we shall see, all observables can be expressed in terms of surface values of Clebsch field.

We neglected viscosity here, but it plays an important role behind the scenes, just like particles interaction in the gas leads to Boltzmann distribution which only depends of the sum of their kinetic energies. The physics behind this distribution is the energy exchange between the particle and the thermostat made of the others. This energy exchange results from interaction, but specific form of this interaction does not affect resulting Boltzmann distribution.

In our case this would be the volume and vorticity exchange between cells due to viscosity effects: cells will split and reconnect in course of dynamics thanks to viscosity, and this would convert micro-canonical distribution $\delta\left(V - V_0\right)$ to the exponential distribution $\exp(-\beta V)$. Viscosity would influence the relaxation time $T \sim \frac{1}{\nu}$ but will drop from the equilibrium distribution in the same way as interaction strength drops from the Gibbs-Boltzmann distribution for ideal gas.

Obviously, the viscosity effects work at the cell boundary. The normal vorticity vanishes there but not the vorticity components along the boundary. With Jacobian vanishing in (17) this would lead to singularity in vorticity $\omega_{\alpha\beta}$ in physical space. Therefore, the dissipation term $\nu\Delta\omega$ in vorticity equation would go to infinity at the boundary, which means it cannot be neglected and results in smooth transition to $\omega = 0$ outside within a thin lawyer.

Note that there is not enough variables in Clebsch field to make all three components of vorticity vanish at the boundary, so the Neumann boundary conditions $n_a\partial_a\phi_{1,2} = 0$ would not help. The vorticity flux outside will not vanish for Neumann boundary conditions, so they are not acceptable.

The normal vorticity vanishes at the boundary, but velocity does not, so that circulation along the boundary can be computed as $\oint_{C\in\partial D} dr_\alpha v_\alpha = \oint_{C\in\partial D}|\psi|^2 d\arg\psi$. Let us make a small deformation of the loop C along the cell boundary. The variation of the circulation Γ_C reduces to vanishing circulation around a little loop δC which belongs to the boundary. Thus, the circulation Γ_C does not change which allows us to shrink the loop to a point if topology permits.

Therefore, these circulations around the handles of the cell are topologically invariant, and in particular, circulation around any loop on a spherical cell equals to zero.

The circulations around the handles of vortex cell is the only possible source of time reversal breaking in three dimensions: as it was analyzed in [1], the other possible invariant vanish. Here is this analysis.

The generic $\Omega-$invariant in d dimensions is

$$\int_D d^d\rho\sqrt{\det\Omega_{ab}} \tag{51}$$

In *even* dimensions $d = 2k$ this invariant reduces to the Pfaffian

$$\int_D d^{2k}\rho\sqrt{\det\Omega_{ab}} = \frac{1}{k!}\int_D \Omega\wedge\Omega\cdots\wedge\Omega = \int_D\frac{\Omega^k}{k!} \tag{52}$$

In two dimensions it would be simply the net vorticity of the cell

$$\int_D d^2\rho\Omega_{12} \tag{53}$$

However, in odd dimensions it vanishes so that there is no $\Omega-$invariant. This is happening because in odd dimensions $d = 2k + 1$ the eigenvalues of anti-symmetric matrix come in pairs $\pm\lambda$ with last odd eigenvalue being zero.

We see that there is a significant difference in the vortex statistics in even and odd dimensions.

Another interesting comment. For odd $k = \frac{d}{2}$ the $\Omega-$invariant is an odd functional of Ω which breaks time reversal invariance. The vorticity stays invariant under space reflection but changes sign at time reversal. This simple local mechanism of the time irreversibility is present only at $d = 4k + 2, k = 0, 1, \ldots$. In three dimensions we live in it is absent.

However, there is another invariant, more subtle one. There is an internal $U(1) = O(2)$ symmetry in this dynamics, corresponding to rotation of 2D vector (ϕ_1, ϕ_2), or, as we prefer to view it, phase transformation of complex field

$$\psi = \phi_1 + \imath\,\phi_2 = |\psi|e^{\imath\,\alpha} \tag{54}$$

$$\Omega = d\phi_1 \wedge d\phi_2 = -\imath\, d\bar{\psi} \wedge d\psi \tag{55}$$

$$\Gamma = \oint \phi_1 \wedge d\phi_2 = -\imath \oint \bar{\psi} \wedge d\psi \tag{56}$$

This internal symmetry can be linked to the topology of the vortex cell by demanding that $|\psi| = R, \psi \in \partial D$. Assuming that boundary value of ψ acquires the phase shift $2n\pi$ when rotated around the handle h we find the circulation for the loop L_h around such handle

$$\Gamma_h = -\imath \oint_{L_h} \bar{\psi} d\psi = R^2 \oint_{L_h} d\alpha = 2\pi w_h R^2 \tag{57}$$

Mathematically, this is homology of sphere S^1 to an orientable surface ∂D with some number of handles.

The parameter R is another integral of motion in our system. Each cell has its own boundary value $|\psi| = R$.

At arbitrary constant $|\psi| = R$ the normal vorticity at the surface will vanish, therefore there will be no flux outside, as we demanded. The circulation around any external loop C will reduce to sum of terms like (57) from all handles surrounding C. (see Fig. 1).

The specific shape of the function $\alpha(u, v)$ where u, v are coordinates parametrizing the boundary, drops from the circulation. It remains the only variable left of Clebsch field.

Also, as noted in [1] we could add such handle term with some coefficient θ for every handle on the cell to the topological part of Hamiltonian

$$H_T = 2\pi R^2\theta \sum_i \sum_h w_h \tag{58}$$

where w_h is the winding number around this handle h for the cell D_i with $|\psi| = R$ at its boundary.

This term manifestly breaks time reversal symmetry. This symmetry would correspond to complex conjugation of ψ, in which case the phase shift (and hence the winding number) would change sign.

The particular phase shifts $2\pi w_h$ for each handle are motion invariants. They are the only variables left representing the Clebsch fields, and we must sum over all these numbers from $-\infty$ to ∞.

As for the boundary values $|\psi| = R_i$ of the Clebsch field, these values must all be equal across the set of the boundaries ∂D_i of the cells. This universality becomes clear if we consider the (viscosity driven) process of splitting the cell in two and inverse process of joining two cells into one.

The net volume stays constant and is simply redistributed between the cells – and this process is local, as it should for the local viscosity effects. At the place of join/split the boundary reconnects but the remote parts do not change (that would require some improbable global movements).

If we split the cell in two, the boundary values of $|\psi|$ would come out the same at both emerging cells, but if we try to join two cells with different values of $|\psi|$ at the boundary there will appear the discontinuity of the surface value of $|\psi|$ at the merging point. This discontinuity would lead to the leak of vorticity which would stop only if the discontinuity disappears.

So, in the following we assume equal value $R_i = R$ for all cell boundaries. This R is the global dimensional parameter to fix the scale of vorticity and therefore velocity. There is also the spatial scale $\beta \sim L^{-3}$ in front of the net volume. The velocity scales as $v \sim R^2\beta^{\frac{1}{3}}$ and the energy flow $\mathcal{E} \sim R^6\beta^{4/3}$.

Let us now check the Liouville equation in presence of the fixed circulation around some loop. The time derivative of the circulation reads

$$\partial_t \Gamma_C[v] = \oint_C dr_\alpha \omega_{\alpha\beta}(r) v_\beta(r) \tag{59}$$

The equilibrium solution for the PDF of circulation must satisfy the equation

$$\partial_t \left\langle \theta\left(\Gamma - \Gamma_C[v]\right)\right\rangle = -\left\langle \delta\left(\Gamma - \Gamma_C[v]\right) \oint_C dr_\alpha \omega_{\alpha\beta}(r) v_\beta(r) \right\rangle = 0 \tag{60}$$

where the averaging $\langle\rangle$ goes over all configurations of vortex cells and Clebsch field inside.

In general, the loop C goes through the cells as well as through the empty space in between cells. The dominant cell configuration in equilibrium will be such that the integral $\oint_{C\in D} dr_\alpha \omega_{\alpha\beta}(r) v_\beta(r)$ vanishes for each cell D.

This will naturally happen if cells all avoid C, in other words if the loop C will be surrounded by an infinitesimal "insulator" of $\omega = 0$ region, like a wire in electric cable[2]. So, the cell can surround C but there is a guaranteed wormhole through the cell making sure $\omega(r) = 0, r \in C$.

The velocity, being nonlocal, is finite everywhere in space, including the loop, so that the circulation $\Gamma_C[v]$ does not vanish. However, it becomes a topological invariant at fixed R.

We cannot prove stability of this stationary solution for the cell configuration for the conditional probability for fixed constant circulation. This remains a conjecture of this theory, to be verified later. The only justification we can give at the moment is the mathematical beauty and simplicity of emerging topological model of developed Turbulence. The distribution of vorticity inside cell is not defined by our theory, but it can be eliminated from all observable quantities (see discussion in the next Section).

If we consider arbitrary Stokes surface bounded by C, the circulation will now reduce to vorticity flux inside all handles being cut by the Stokes surface. Another way of saying this is that circulation will add up from the vorticity flux through all the handles surrounding C.

$$\Gamma_C = 2\pi R^2 \sum_{h:C\in h} \pm w_h \tag{61}$$

The signs here are positive/negative for equal/opposite orientations of C and the loops L_h for each handle. The variable R is continuous so that Γ_C remains a continuous variable.

Clearly, the time reversal (symmetry between Γ and $-\Gamma$) is broken by the θ terms.

Remarkable feature of this theory is that the Clebsch field is a compact scalar field on the surface of each cell. This is EXACTLY the same problem as in compactification of one-dimensional Bosonic string [9] with α field denoted as string X on a circle S^1 mapped to a manifold $M_g = \partial D$

$$Z = \int [dg_{\alpha\beta} R dX] \exp\left(-\frac{R^2}{4\pi}\int_{M_g} d^2\xi \sqrt{g} g^{\alpha\beta}\partial_\alpha X \partial_\beta X\right) \tag{62}$$

The resulting partition function (apart from Liouville field for the conformal metric) was calculated in the 80-ies:

$$Z_g[C] = \int_{\mathcal{M}_g} dm D(m) R \sum_{m_i,n_i} \exp\left(-R^2 I(M_g)\right) \tag{63}$$

$$I(M_g) = \pi\left(\boldsymbol{m} + \boldsymbol{n}\tau\right)^\dagger \tau_2^{-1}\left(\boldsymbol{m} + \boldsymbol{n}\tau\right) + \boldsymbol{m}\boldsymbol{\Phi}[C] + \boldsymbol{n}\boldsymbol{\Psi}[C] \tag{64}$$

where

$$\tau_{ij} = \tau_{1ij} + \imath\, \tau_{2ij} \tag{65}$$

is the complex symmetric period matrix. It is parametrized by $3g-3$ modular parameters $m \in \mathcal{M}_g$ (see references in [9]). The integer vectors $\boldsymbol{m} = m_1 \dots m_g, \boldsymbol{n} = n_1 \dots n_g$ are the winding numbers around a, b cycles in so called

[2]This vanishing vorticity takes place at the microscopic (i.e. viscous) scales. Effective vorticity, being averaged over volume at inertial range of scales, would be finite. We elaborate this idea later in the framework of the lattice model.

symplectic Hodge basis (see Fig 9).

$$\oint_{a_i} dX = 2\pi m_i \tag{66}$$

$$\oint_{b_i} dX = 2\pi n_i \tag{67}$$

$$i = 1 \dots g. \tag{68}$$

So, the winding numbers w_h consist of these n, m vectors. Explicit solution for $X = \Re F(z)$ on the Riemann surface for M_g can be found in [9]. We only need the resulting minimal Action $I(M_g)$. This partition function is invariant under the $Sp(2g, \mathbb{Z})$ transformations, simultaneously acting on (m, n) and τ. In particular, for $g = 1$ (torus) there is an $SL(2, \mathbb{Z})$ transformation

$$\tau \to (a\tau + b)/(c\tau + d), \tag{69}$$

where $ad - bc = 1$ (therefore $\gcd(a, b) = \gcd(c, d) = 1$). The classical Action $I(M_g)$ stays invariant if the winding numbers transform as

$$n \to w_1 = na + mc, m \to w_2 = md + nb; \tag{70}$$

In the frame where $n = 0, m = N$ after an arbitrary group transformation

$$n = Nc, m = Nd \tag{71}$$

We observe that $N = \gcd(n, m)$ represents an invariant definition of the winding number.

So, the $SL(2, \mathbb{Z})$ invariant definition [10] of the circulation around a handle of a torus

$$\Gamma = 2\pi R^2 N;\ N = \gcd(m, n) \tag{72}$$

The sum over all values of m, n in case of fixed circulation $\Gamma = 2\pi R^2 N$ will be restricted by fixed $N = \gcd(m, n)$:

$$\sum_{m,n:\gcd(m,n)=N} \tag{73}$$

In general case vectors length g $\mathbf{\Phi}[C], \mathbf{\Psi}[C]$ are made of Lagrange multipliers for Γ and θ terms combined. They depend of the loop C because dependent of C they surround some subset of handles of ∂D with various orientations. The integral in (62) is performed over the moduli space $\mathcal{M}_g$ of M_g and the sum extends to all integers n_i, m_i.

In addition there is a usual Liouville effective Lagrangean for φ

$$H_\varphi = \int d^2 z \frac{1}{2} (\nabla\varphi)^2 + a e^{\varphi} + Q\varphi \tag{74}$$

where Q is "central charge" yet to be determined. The Clebsch-string field $\psi = Re^{\imath X}$ also adds to the central charge after functional integration,

This leads to the following partition function (including Lagrange multipliers for circulation Γ) at fixed configuration of vortex cells $\{D_i\}$

$$Z(C|\{D_i\}) \propto \int_{\mathcal{M}_g} dmD(m) R \exp\left(-\frac{1}{2}\log \text{Det}\ \left(-\hat{L}(\tau)\right)\right) \int (D\varphi) \exp\left(-H_\varphi\right) \sum_{m_i, n_i} \exp\left(-R^2 \sum_D I(M_g)\right) \tag{75}$$

The Bosonic determinant Det $\left(-\hat{L}(\tau)\right)$ on a Riemann surface was computed in String Theory [11], [12]. It depends on τ but not on the winding numbers m, n. The integral $\int_{\mathcal{M}_g} dmD(m)R$ stands for integration over $Sp(2g, \mathbb{Z})$ invariant measure in moduli space.

In particular, for $g = 1$ (torus) invariant measure [9]

$$\int_{\mathcal{M}_1} dmD(m) = \int_{-\frac{1}{2}}^{\frac{1}{2}} d\tau_1 \int_{\sqrt{1-\tau_1^2}}^{\infty} \frac{d\tau_2}{\tau_2^2} \tag{76}$$

and determinant [10]

$$\text{Det}\ \left(-\hat{L}(\tau)\right) = \tau_2 \left|\eta(\tau_1 + \imath\, \tau_2)\right|^4 \tag{77}$$

where $\eta(\tau)$ is Dedekind η function.

We leave to the experts this hard mathematical problem of computation of that integral in general case. Similar sums/integrals for multi-instantons were computed for two- dimensional sigma model and supersymmetric four dimensional YM theories.

So, at given topology of the set of cells and their topology with respect to the loop C this partition function is calculable analytically! The unknown shapes of the cell boundaries in parameter space as well as physical space dropped from this formula, only the Liouville field, period matrix and winding numbers are left.

Note the the exponential is always decreasing as $I(\partial D)$ is positive quadratic form of the winding numbers which grows faster than linear θ terms. Therefore at large winding numbers this distribution converges.

Note that we reduced this theory to one dimensional Bosonic string compactification problem just because we restricted ourselves to circulations. The velocity field inside cells is a much more complex object which we cannot study by these methods. On the other hand, as we discuss at the end of this paper, all observables which can be expressed in correlations of vorticity can be reduced to this topological theory.

Now, the reader may wonder how could the Bosonic String Theory exist in three dimensions. The theory based on Liouville field as well as numerical simulations, all show that there is no continuum limit for the random surfaces in three or four dimensions. These surfaces degenerate into branched polymers so they would not serve our purposes.

Here is an important difference which could save the day. Our surfaces are not the ordinary free surfaces of the String Theory. They are rather boundaries of three dimensional cells. As such these surfaces are avoiding each other as well as themselves.

The String Theory still applies to the Clebsch field dynamics at fixed shape of the cell. This compactification and this functional integral over X and moduli do not show anything pathotological, they are calculable and finite.

As for sum/integral over cell shapes, it is NOT described by any known string theory. As we suggest in the next section, this surface dynamics is isomorphic to that of three dimensional Ising model.

4 Vortex Cells and Ising Model

This statistics of self avoiding drops with distribution $P = \exp(-\beta V - \gamma S)$ sounds familiar. Where did we hear that tune? But of course! Ising model in magnetic field. The Ising Hamiltonian on a 3D lattice,

$$H_I = h\sum_r \Theta(\sigma(r)) + \kappa \sum_{\langle r,r'\rangle} \Theta(-\sigma(r)\sigma(r')) \tag{78}$$

with $\langle r, r'\rangle$ denoting lattice neighbors and

$$\Theta(\sigma) = \frac{1+\sigma}{2} \tag{79}$$

being projector to $\sigma = 1$, leads to partition function (we measure all distances, areas and volumes in lattice spacing units)

$$Z_I = \sum_{\{\sigma\}} \exp(-\beta H_I) \tag{80}$$

$$= \sum_i \sum_{D_i} \exp\left(-\beta \sum_i (hV_i + \kappa S_i)\right) \tag{81}$$

where D_i are drops of the phase $\sigma = 1$ in the background of $\sigma = -1$ with volumes V_i and surface S_i and the sum goes over all partitions of space in to two phases, i.e. over all shapes and positions of non-overlapping self-avoiding drops D_i. The Ising model in three dimension exists and has the continuum limit, meaning that these cells become macroscopic and lattice artefacts go away near critical point. Ising model phase boundaries do not degenerate to branched polymers of low-dimensional String Theory.

We shall associate the spin variables σ with centers of cubic cells of the body-centered cubic lattice, i.e. vertices of the dual cubic lattice (see Fig. 2).

This way the phase boundaries are made of the squares of original lattice. For example, a single variable $\sigma = 1$ inside the background of $\sigma = -1$ occupies the cubic cell with six squares as boundary, i.e. $V = 1, S = 6$. Two adjacent $\sigma = 1$ cells have $V = 2, S = 10$ etc. The bonds $\langle r, r'\rangle$ between centers of neighboring cells are dual to the square boundary separating them (See Fig. 3).

One may wonder how the discrete Ising variables can substitute for the continuous coordinates $X_\alpha(\rho)$ of the Lagrange dynamics. The key to understand it is the conservation of the volume.

Let us divide the initial ρ space into cubic cells of our lattice and note that the volume conservation means that the cells initially filled with vorticity just move around in a flow without changing their volume. In the lattice approximation this motion is a discrete mapping of initial occupied cells ρ_i to the cells $\rho'_i = X(\rho_i)$ at later moments. This can be achieved as a series of moves $\sigma = 1$ at one cell to $\sigma = 1$ at its neighbor with simultaneous flip from $\sigma = 1$ to $\sigma = -1$ at initial one. So, sequences of spin flips on the lattice can reproduce the discrete version of Lagrange dynamics.

Now let us recall our hidden Clebsch variables. This is complex field $\psi(r)$ associated with phase boundaries.

The computer implementation of this body-centered lattice is to have an integer grid in 3 dimensions and place Ising spins in odd cites r_o (with all 3 coordinates odd) and Clebsch fields in even cites r_e (all 3 coordinates even). The neighbours are defined as nearest points with the same parity, i.e. spaced by ± 2 by one coordinate. The corners of the square between two neighbor spin cites r_o, r'_o in direction μ has $r_{e,\mu} = \frac{1}{2}\left(r_{o,\mu} + r'_{o,\mu}\right)$ and 4 possible values $r_{e,\nu} = r_{o,\nu} \pm 1$ of remaining two coordinates. So, the odd and even lattices are dual to each other.

We also have to define lattice analog of circulation and vorticity in such a way that Stokes theorem would hold on the lattice and topological numbers would become Euler characteristics on a polygonal surface.

Let us start with circulation. We can define it in polar coordinates $\psi = Re^{\imath\,\phi}$:

$$\Gamma_C = \oint_C |\psi|^2 d\phi \Rightarrow R^2 \sum_i (\phi_{i+1} - \phi_i) \tag{82}$$

This definition has important additivity property

$$\Gamma_{L_1+L_2} + \Gamma_{L_2^{-1}+L_3} = \Gamma_{L_1+L_3} \tag{83}$$

where the first closed loop $C_{12} = L_1 + L_2$ and the second one $C_{23} = L_2^{-1} + L_3$ have common path L_2 traversed in opposite directions, such as the circulations of two adjacent squares on the lattice. Each term in our lattice sum (82) changes sign when traversed in opposite direction.

Therefore the term from the shared link cancels in the sum of circulations of adjacent squares so that we are left with 6 terms corresponding to perimeter of the two-square surface. Pooling together the elementary squares terms for arbitrary lattice surface made of squares we find that all inner links cancel so that we are left with the circulation (82) for the perimeter.

The definition of the vorticity consistent with this definition of circulation is the same as definition of the field tensor in lattice gauge theory. Vorticity components ω_{ab} are defined as circulation around elementary squares in ab plane.

$$\omega_{ab}(\square_{ab}) = R^2 \sum_{i=1}^{4} (\phi_{i+1} - \phi_i) \tag{84}$$

where r_1, r_2, r_3, r_4 are the corners of the square $\square$ in cyclic order.

With this definition of vorticity the total vorticity flux through the closed surface would cancel as it should, because all contributions of links would enter twice with opposite sign. In our theory there is a stronger requirement, namely that every term in this flux must vanish as the normal component of vorticity vanishes at the cell boundary.

By the same reasons the circulation around the handle (representing vorticity flux through this handle) is topologically invariant on the lattice as well as in continuous theory. By adding elementary squares (each with vanishing circulation) to this loop we can deform this loop without changing its circulation. In case these deformations cannot shrink the loop to a point we get topological invariant (winding number around this handle).

Now, these winding numbers are all what is left in our theory from the Clebsch variables. We have to compute the topology (set of handles and the way they are represented on a Fundamental Polygon by gluing sides) and then we get the weight for a given configuration of cells.

The topology (number of handles $H = g$) of this surface can be defined by the Euler theorem for the polygonal surface. In case of P disjoint pieces the Euler characteristic is additive, so

$$N_0 - N_1 + N_2 = 2P - 2H \tag{85}$$

In addition, on a quadrilateral closed surface each pair of faces shares unique edge so we have $N_1 = 2N_2$ therefore

$$H = P + \frac{1}{2}(-N_0 + N_1 - N_2) = P + \frac{1}{2}(N_2 - N_0) \tag{86}$$

the number of faces N_2 is expressed in Ising spins as follows

$$N_2 = \sum_{\langle r_o, r'_o \rangle} \Theta(\sigma(r_o))\Theta(-\sigma(r'_o)) \tag{87}$$

The sum goes over all neighboring odd lattice cites $\langle r_o, r'_o \rangle$ (i.e. r_o, r'_o differing by ± 2 in one of components) and the Θ factor select only those belonging to different phases.

The number of connected pieces P is computed in Appendix by the algorithm 2 which uses recursive labeling algorithm 1. As an output of this algorithm all points in each connected piece are labelled by unique label $l(r_o) = 1 \dots P$ on the odd lattice. The number N_0 of vertices is computed in Appendix by algorithm 3, using these labels $l(r_o)$. Note that in case of cells touching by corners (see Fig. 4) or by sides (see Fig. 5) the vertices are counted twice, in other words, these touching cubes are treated as disjoint pieces of surface. This is because we count connectivity by the neighborhood on odd lattice, which corresponds to neighbors sharing a face (see Fig 3). Sharing corners or edges is not counted in connectivity graph.

From the point of view of vorticity flux, this touching vertex or touching side does not connect these cubes, as the cross section area is zero. So, there is no vorticity flux from one cube to another, therefore these common vertices and these common sides should be counted twice, as parts of different cells.

We leave aside the computational efficiency of this algorithm – apparently, the Monte Carlo simulation would use incremental algorithm, with flipping one spin at a time and finding corresponding differences $\Delta P, \Delta N_0, \Delta N_2$.

The circulation Γ can also be expressed in terms of our Ising+Clebsch variables as a sum over all handles surrounding C

$$\Gamma_C = 2\pi R^2 \sum_{h:C\in h} \pm w_h \tag{88}$$

The signs here depend upon relative orientation of the loop and surrounded handles. The algorithm for computation of Γ_C is presented in Appendix.

As discussed above there are also topological terms for every handle on the cell which represent the (conserved) net flux of vorticity inside the handle. It is equivalent to circulation of any loop L surrounding this handle from outside, where vorticity vanish, but velocity is present.

There is one more important requirement, leading to extra terms, namely requirement that the external loop C in definition of circulation cannot go inside the cell. This is taken care of by projection factor

$$P[C] = \prod_{r_o \in C} \Theta(-\sigma(r_o)) \tag{89}$$

with the convention that the loop C goes through the vertices of the odd lattice, i.e. the centers of the cells.

Let us check that all components of vorticity vanish at the loop as they should for the circulation to be conserved and the loop equation to be valid. A cube of the even lattice L_e corresponding to a dual cite $r_o \in C$ has 6 square sides, at least two of which belong to C and therefore to the phase $\sigma = -1$. Circulation around these squares and therefore their ω vanish in this phase.

The remaining sides may be boundaries with the $\sigma = 1$ phase but in that case the circulation around that square vanishes due to our boundary condition. Therefore, all components of vorticity on the boundary of every cube belonging to C vanish as it is needed for the circulation conservation.

Remarkable feature of this Ising+Clebsch model is that it is calculable, at least in low temperature expansion ($u = \exp(-\beta h), v = \exp(-\beta\kappa)$):

$$Z_C(u, v, \Gamma, \theta, \gamma) = \sum_i \sum_{D_i \cap C = \emptyset} u^{\sum_i V_i} v^{\sum_i S_i} Z(\Gamma, C|\{D_i\}) \tag{90}$$

Here $Z(\Gamma, C|\{D_i\})$ was defined in a previouis section (75) with Lagrange multipliers for Γ. The practical way of computing it is to draw arbitrary Stokes surface bounded by edges belonging to cubes dual to odd lattice points in C and count the number w_h of intersections of this surface by handles of our drops. These numbers should be taken with proper signs depending on mutual orientation. If the same handle intersects the surface twice, these two numbers cancel each other. As a result this $\Gamma_C = 2\pi R^2 \sum_h (\pm w_h)$.

In general, there will be asymmetry between positive and negative Γ due to the topological θ terms. We see that

$$\operatorname{sign}\Gamma = \operatorname{sign} \sum_{h:C\in h} \pm w_h \tag{91}$$

where the sign in front of winding number w_h depends of relative orientation of the Stokes surface for C and the surface of the boundary D_i of the vortex cell.

All the winding numbers here for each handle on each cell can be computed for any configuration of Ising spins $\sigma(.)$ on the odd lattice L_o using algorithms which we describe as a pseudo-code in Appendix.

So, at fixed set of cells we get asymmetric exponential distribution in qualitative agreement with numerical experiments [7]. This is encouraging, though much more work is required before we can get any quantitative predictions from this topological Ising model. This would be a very interesting numerical project which we postpone for future.

5 Area Law, Clebsch Confinement and Multi-Fractals

Let us now consider tails of circulation PDF. The loop is large compared to the typical size of vortex cells but the cell is surrounding this loop. The dominant (classical) configuration would minimize the volume at given large circulation. In the simplest spherical topology of the cell this would become a thin vortex sheet around minimal surface, just as conjectured in the old paper [6] and developed further in my recent papers.

Why not just one toroidal thin cell around the loop like insulator around electric wire in a cable? Because in that case the circulation would not be as large as possible, but rather proportional to the perimeter of the loop. To make this circulation as large as possible at given volume we would need a pancake with viscous thickness around this minimal surface. Actual vorticity distribution inside this pancake is nontrivial, and has to be found from the loop equation in the classical limit.

In fact, as it was discussed in the previous section, the topology of this pancake must be more complex. The loop C inside must be surrounded by toroidal empty space (wormhole), as the vorticity cells by construction avoid the loop. (see Fig. 6).

The alternative cable-shaped cell would in fact look like toroidal wormhole in toroidal vorticity cell (see Fig. 7).

Note that in both cases there is at least one handle in the topology of the vortex cell, which necessarily leads to time reversal symmetry breaking by the θ terms described in the previous section.

Which one of these two geometries is realized in isotropic Turbulence? My recent work on loop equations favors the pancake, but it is ultimately up to future numerical experiments to answer this question.

The main conjecture is that vorticity does not spread all over the space but is confined to collection of cells with sealed boundaries not letting vortex lines go outside and spread all over the space. We know [3] that vorticity takes less than whole space – vorticity-filled region has fractal dimension $d_f \sim 2 + 1/3$. The fact that it is less than three means that the net volume of the vortex cells can serve as the dynamic variable in place of the Hamiltonian. The total energy grows faster than volume because of the infrared divergency whereas the total cell volume is by construction bounded by volume.

On top of that macroscopic picture there may be handles at microscopic scale, with their time-reversal breaking terms. We are now considering classical limit, when these fluctuations are neglected, or, better accounted for as next correction to the WKB expansion as fluctuations around minimal surface and mean vorticity field. Loop equations provide the framework for such WKB expansion. The pure exponential law could get modified to exponential of some power of Γ as a result of these fluctuations.

The Clebsch variables inside this vorticity sheet would display themselves through the composite field Φ in (4). Explicit relation between these fields is not clear at present. This relation could be non-local and implicit.

As for the fact that mean Γ in the tails of PDF grows only as $A_C^{0.5}$ rather than linearly, this must come from the fact that mean vorticity inside the cell are not aligned, but rather have finite correlation length. Thus mean vorticity density decreases as $A_C^{-0.5}$ because of this lack of global alignment.

This is one of remaining problems for future study, as well as the nontrivial power μ of Γ in observed PDF tails (3).

When we compare the circulation statistics with that of velocity field in this vortex cell approach we observe striking difference, which explains lack of multi-fractal distribution for the circulation. Namely, the circulation statistics only depends of volumes of the vortex cells and the topology of the Clebsch field. The velocity statistics manifestly depends of the vorticity (i.e. Clebsch field) distribution inside each cell, but circulation Γ_C adds up from constant topological terms for each handle surrounding C.

[3] This estimate [13] followed from Biot-Savart integral assuming some region of dimension d_f occupied by vorticity $v \sim r^{d_f-2} \sim r^{\frac{1}{3}}$

Dynamic vorticity flow inside cells all reduce to these quantized topological terms. This magic happens because of Stokes theorem and lack of vorticity flow outside the cells. The dynamical flux of Clebsch-defined vorticity through the Stokes surface cutting the cell reduces to the Clebcsh winding numbers around intersected handles times the boundary value $|\psi|^2 = R^2$. This makes this winding number proportional to circulation and leads to the exponential decay of circulation PDF provided the effective winding number Hamiltonian grows linearly with w_h.

Velocity on the other hand adds up from long-range Biot-Savart contributions (14) from all cells in the turbulent flow, each with its own spatial scale. This could naturally lead to multi-fractal distribution of local vorticity: in [1] it was argued that random surface approach with string theory methods leads to Kolmogorov-Obukhov model of fluctuating energy flow resulting in quadratic index $\zeta(n)$. The actual PDF for local vorticity and velocity differences must be measured in the above Ising model.

In numerical experiments a transition scale was observed corresponding to relatively large Reynolds numbers. The Kolmogorov energy cascade with $|\omega| \sim r^{-\frac{2}{3}}$ works up to this transition scale, after which multi-fractal laws kick in [14].

In our theory this intermediate scale would correspond to typical size of drops. As scales much smaller than drop size one could work in the conventional theory, with viscosity filling whole space, and neglect all the boundary effects of the cell. In effect, there is only one cell in this region, taking the whole space. In this approximation the global formulas for velocity as $v = -\imath\,\bar{\psi}\nabla\psi + \nabla\Phi$ would be valid, and the Fourier transformation would be valid in absence of the boundaries.

The mean field approximations of Yakhot and Zakharov [8] leading to $5/3$ would also make sense [4], with ω having scaling dimension $-\frac{2}{3}$ coming as result of some OPE for product of $e^{abc}\partial_a X_\alpha \partial_b \bar{\psi}\,\partial_c\psi$. Obviously, this is not a conserved current of some CFT. Naively, the free field ψ in 3 dimensions would have scaling dimension $-\frac{1}{2}$, so the normal dimension for ω would be -3 by power counting without taking into account unknown dimension of $\partial_a X_\alpha$.

The strong anomaly in scaling dimension of vorticity indicates some interaction at small distances, which we still do not know about. The Hamiltonian $\frac{1}{2}v^2$ corresponds to quartic interaction of the Euler Clebsch fields, which may be an indication for some unknown CFT describing these small scale phenomena.

At larger scales the Clebsch correlation grows as $r^{\frac{4}{3}}$ by naive power counting (we do not know anomalous dimensions of Clebsch fields) so that the boundary effects for the vorticity drops would become important, and presumably these effects lead to multi-fractal scaling for vorticity.

The above approach with circulation PDF allows to obtain arbitrary correlation functions of vorticity taking special case of small loops. For example the correlation $\langle\omega(r_1)\omega(r_2)\rangle$ can be considered as a limit of double loop correlator $\langle\Gamma_{C_1}\Gamma_{C_2}\rangle$, with loops shrinking to points r_1 and r_2. It would pinch one or more vortex cells in two places (see Fig.8). As the cells cannot intersect these loops, only the vortex structures with a handle surrounded by both loops will contribute to a correlator.

As for velocity difference moments, those are expressible in terms of vorticity correlators by an ordinary Biot-Savart integrals in physical space, so the above model provides computational method to study these moments with our Ising+Clebsch model (see Fig. 8).

6 Conclusion

In conclusion, the analysis of Hamiltonian dynamics of Turbulence with the same reasoning which led from Liouville Equation to the Gibbs distribution, after taking into account all local and global symmetries of this dynamics in Clebsch variables, leads to the statistical model of vortex cells as drops of one phase of the Ising model in magnetic field with free massless complex Clebsch field $\psi, |\psi| = \text{const}$ on the surface of these drops. This surface Clebsh statistics is exactly equivalent to solved problem of S^1 compactification of Bosonic String. The θ terms in that theory would lead to time reversal breaking, i.e. asymmetry of the circulation PDF. This circulation is reduced to superposition of winding numbers of Clebsch string around handles of vortex cells. The tails of this PDF come as superposition of exponential terms coming from vorticity cells inside the large loop C. This naturally leads to the minimal surfaces as the minimal volume cells covering the loop.

There are many details which need further study and maybe revision. The integration over moduli space $\mathcal{M}_g$, the explicit form of Bosonic determinant $\hat{L}(M_g)$, the simulation of the Ising model. Combined work of fluid dynam-

[4]Note added. I learned from interesting talk of T. Matsuzawa and W. Irvine [15], that experimentally observed vortex blobs, are indeed not leaking and that vorticity inside a blob approximately obeys Kolmogorov scaling law. That work validates my picture of confined vorticity blobs and their statistics.

ics/turbulence theorists and numerical simulation, theoretical insights from string theorists and pure mathematicians and also input from experts of phase transitions and conformal bootstrap in Ising model are all welcome.

7 Acknowledgements

I am grateful to Sergey Dubovsky, Kartik P. Iyer, Sasha Polyakov, Yakov Sinai, Katepalli R. Sreenivasan and Victor Yakhot for useful discussions of Physics of my work. Mathematical structures were explained to me by Nikita Nekrasov, Massimo Porrati and Ed Witten.

This work is supported by a Simons Foundation award ID 686282 at NYU.

References

[1] A. A. Migdal. Turbulence as statistics of vortex cells. In V.P. Mineev, editor, *The First Landau Institute Summer School, 1993: Selected Proceedings*, ... @Landau Institute Summer School: Institut Teoretičeskoj Fiziki Imeni L.D. Landau, pages 178–204. Gordon and Breach, 1993. ISBN 9782884491389. URL https://arxiv.org/abs/hep-th/9306152v2.

[2] Alexander Migdal. Universal area law in turbulence, 2019. URL https://arxiv.org/abs/1903.08613.

[3] Alexander Migdal. Scaling index $\alpha = \frac{1}{2}$ in turbulent area law, 2019. URL https://arxiv.org/abs/1904.00900v2.

[4] Alexander Migdal. Exact area law for planar loops in turbulence in two and three dimensions, 2019. URL https://arxiv.org/abs/1904.05245v2.

[5] Alexander Migdal. Analytic and numerical study of navier-stokes loop equation in turbulence, 2019. URL https://arxiv.org/abs/1908.01422v1.

[6] Alexander Migdal. Loop equation and area law in turbulence. In Laurent Baulieu, Vladimir Dotsenko, Vladimir Kazakov, and Paul Windey, editors, *Quantum Field Theory and String Theory*, pages 193–231. Springer US, 1995. doi: 10.1007/978-1-4615-1819-8. URL https://arxiv.org/abs/hep-th/9310088.

[7] Kartik P. Iyer, Katepalli R. Sreenivasan, and P. K. Yeung. Circulation in high reynolds number isotropic turbulence is a bifractal. *Phys. Rev. X*, 9:041006, Oct 2019. doi: 10.1103/PhysRevX.9.041006. URL https://link.aps.org/doi/10.1103/PhysRevX.9.041006.

[8] Victor Yakhot and Vladimir Zakharov. Hidden conservation laws in hydrodynamics; energy and dissipation rate fluctuation spectra in strong turbulence. *Physica D: Nonlinear Phenomena*, 64(4): 379 – 394, 1993. ISSN 0167-2789. doi: https://doi.org/10.1016/0167-2789(93)90050-B. URL http://www.sciencedirect.com/science/article/pii/016727899390050B.

[9] Amit Giveon, Massimo Porrati, and Eliezer Rabinovici. Target space duality in string theory. *Physics Reports*, 244(2):77 – 202, 1994. ISSN 0370-1573. doi: https://doi.org/10.1016/0370-1573(94)90070-1. URL http://www.sciencedirect.com/science/article/pii/0370157394900701.

[10] Nikita Nekrasov. Compact boson in two dimensions. Private Email, 20/11/2019.

[11] Luis Alvarez-Gaumé, Gregory Moore, and Cumrun Vafa. Theta functions, modular invariance, and strings. *Communications in Mathematical Physics*, 106(1):1–40, Mar 1986. ISSN 1432-0916. doi: 10.1007/BF01210925. URL https://doi.org/10.1007/BF01210925.

[12] Leon A. Takhtajan. Free bosons and tau-functions for compact riemann surfaces and closed smooth jordan curves. current correlation functions. *Letters in Mathematical Physics*, 56(3):181–228, Jun 2001. ISSN 1573-0530. doi: 10.1023/A:1017999407650. URL https://doi.org/10.1023/A:1017999407650.

[13] Alexander Migdal. Fractal dimension of vorticity. Talk at ACM seminar in Princeton University, 1989.

[14] Victor Yakhot and K.R. Sreenivasan. Towards a dynamical theory of multifractals in turbulence. *Physica A: Statistical Mechanics and its Applications*, 343:147 – 155, 2004. ISSN 0378-4371. doi: https://doi.org/10.1016/j.physa.2004.07.037. URL http://www.sciencedirect.com/science/article/pii/S0378437104010593.

[15] T. Matsuzawa and W. Irvine. Realization of confined turbulence through multiple vortex ring collisions. Talk at the Flatiron Conference "Universality Turbulence Across Vast Scales", 03/12/2019.

8 Appendix. Algorithms

In the following the odd lattice L_o is defined as collection of 3 -dimensional integer vectors with all 3 components being odd integers from 1 to $2L+1$. Periodicity in each of 3 direction is implied. Same for the even lattice except the coordinates are even integers from 0 to $2L$.

These two lattices are dual to each other with k dimensional object (point, edge,square,cube) on one lattice being dual to $3-k$ dimensional object (cube,square,edge,point) on the other lattice. The connectivity matrix connects points separated by ± 2 on one of 3 coordinates, which means connectivity by edge. On the dual lattice the cubes are connected by edges, dual to cubes faces.

The number of connected pieces P is expressed in Ising spins by the following algorithm 2 which uses recursive labeling algorithm 1. The number N_0 of vertices can be described by algorithm 3, using previously found labels $l(r_o)$ on odd lattice. The array $\sigma(r_o)$ is changed inside these calls and eventually all $\sigma(r_o)=-1$ at the exit of algorithm. Thus, the copy of actual array of Ising spins σ must be passed to Algorithm 2.

Algorithm 1 Recursive Label Algorithm

procedure RECURSIVELABEL($\&S, \&\sigma(.), \&l(.), M, r_o$)
  $l(r_o) \leftarrow M$ ▷ Label r_0 with M
  $S \leftarrow S-1$
  $\sigma(r_o) \leftarrow -1$
  if $S>0$ **then**
    for $a \in (\pm 2, \pm 2, \pm 2)$ **do** ▷ these are 8 links to neighbors on L_o
      $r'_o \leftarrow r_o + a$
      if $\sigma(r'_o) == 1$ **then** ▷ label all $\sigma == 1$ neighbors
        RECURSIVELABEL$(S, \sigma(.), l(.), M, r'_o)$
      end if
    end for
  end if
end procedure

Algorithm 2 Connected Components Algorithm

procedure COUNTCOMPONENTS$(L_o, \sigma(.))$ ▷ Count pieces, using spin array $\sigma(r_o), r_o \in L_o$
  Define $l(r_o)$ on odd lattice L_o ▷ Array $\sigma(.)$ is passed by value, not by reference, because it is changed inside
  $S \leftarrow 0$ ▷ number of $\sigma == 1$ states
  for $r_o \in L_o$ **do**
    $l(r_o) \leftarrow 0$
    if $\sigma(r_o) == 1$ **then**
      $S \leftarrow S+1$
    end if
  end for
  $M \leftarrow 1$
  for all $r_o \in L_o$ with $\sigma(r_o) == 1$ **do**
    if $S == 0$ **then**
      break
    end if
    RECURSIVELABEL$(S, \sigma(.), l(.), M, r_o)$ ▷ $S, \sigma(.), l(.)$ are changed here
    if $S>0$ **then**
      $M \leftarrow M+1$
    end if ▷ label all neighbors by M recursively
  end for
  return M ▷ $M =$ number of connected components, and $l(r_0)$ are all labelled
end procedure

Algorithm 3 Vertex Count Algorithm

procedure COUNTVERTICES($l(.), L_e, L_o$) ▷ count vertexes using labels and connectivity matrix
  Define $m(r_e), n(r_e)$ on even lattice L_e
  for <all $r_e \in L_e$ > **do**
    $m(r_e) \leftarrow 0, n(r_e) \leftarrow 0.$
  end for
  for <every link $\langle r_o, r'_o \rangle \in L_o$ with $l(r_o) > 0, l(r'_o) == 0$, dual to square $\square \in L_e$> **do**
    for <every one of 4 corners r_e of $\square$> **do** ▷ These corners belong to even lattice
      if $m(r_e) == 0$ **then** ▷ first encounter, count once
        $m(r_e) \leftarrow l(r_o),$
        $n(r_e) \leftarrow 1,$
      else ▷ one of later encounters, count twice if different piece
        if $m(r_e) \neq l(r_o)$ **then**
          $n(r_e) \leftarrow 2$ ▷ only two $\sigma == 1$ cubes could touch by corner or edge
        end if
      end if
    end for
  end for
  $N \leftarrow 0$
  for <all $r_e \in L_e$ > **do**
    $N \leftarrow N + n(r_e).$
  end for
  return N ▷ vertexes double-counted at touching cells
end procedure

Once the labels $l(r_o)$ are known the circulation Γ_C for arbitrary loop on the odd lattice can be computed. We restrict ourselves to a simple loop which is a boundary of some orientable surface S_C with topology of a disk. We further assume that this surface is known as collection of squares $\square$ on an even lattice L_e

$$S_C = \uplus \square \in L_e \tag{92}$$

Let us outline the algorithm of computing the net flux Γ through S_C. The details of this algorithm will be worked out in subsequent paper.

We use the Algorithm 4 to label all intersections of our cells with S_C.

Algorithm 4 Count Intersections Algorithm

procedure COUNTINTERSECTIONS($L_o, \&k(.), l(r_o), C = [r_1, \dots r_N]$)
  for each $\square \in S_C$ **do**
    $k(\square) \leftarrow 0.$
  end for
  for each $\square \in S_C$ such that the dual link $\langle r_o, r'_o \rangle$ has $l(r'_o) == l(r_o), l(r_o) > 0$ **do**
    $k(\square) \leftarrow l(r_o).$
  end for
  COUNTFLUX($L_o, S_C, l(.)$)
end procedure

In general there will be several connected components (cross sections) of the squares with the same index $k(\square)$.

The number of these connected components is obtained by the same recursive labelling algorithm we had for cubes, except this times we label with the same number each of 4 squares on S_C sharing one side with initial one Algorithm 6 and 5.

The problem of computation of the circulation is thus reduced to that of the winding numbers of handles on our cells. This problem was discussed above. One should build the Fundamental Polygon for the surface ∂D and associate the numbers n_i with its sides.

The handles are associated with pairs of sides $h \Rightarrow (i, j)$ and winding numbers are given by $W(h) = n_i - n_j$ when the loop γ crosses the pair of these glued sides.

More explicit algorithm will be presented elsewhere.

Algorithm 5 Recursive Label Algorithm 2

procedure RECURSIVELABEL2($S_C, \&S, \&k(.), \&i(.), M, \square$)
  $i(\square) \leftarrow M$ ▷ Label $\square$ with M
  $S \leftarrow S - 1$
  if $S > 0$ **then**
    for all $\square' \in S_C$ sharing edge with $\square$ **do**
      if $k(\square') == k(\square) \& i(\square') == 0$ **then**
        RECURSIVELABEL2($S_C, S, k(.), i(.), M, \square'$)
      end if
    end for
  end if
end procedure

Algorithm 6 Count Flux Algorithm

procedure COUNTFLUX($L_o, S_C, k(.), i(.)$)
  $S \leftarrow 0$ ▷ number of $k(\square) > 0$ states
  for $\square \in S_C$ **do**
    $i(\square) \leftarrow 0$
    if $k(\square) > 0$ **then**
      $S \leftarrow S + 1$
    end if
  end for
  $M \leftarrow 1$
  for each $\square \in S_C$ such that $k(\square) > 0$ **do**
    RECURSIVELABEL2($S_C, \&S, \&k(.), \&i(.), M, \square$)
    if S >0 **then**
      $M \leftarrow M + 1$
    else
      break
    end if
  end for
  $Y = \emptyset$ ▷ Empty hash table of integer ⇒ set of squares $\square$
  for each $\square \in S_C$ such that $i(\square) > 0$ **do**
    if $k(\square) \in Y$ **then**
      $Y[k(\square)] \leftarrow Y[k(\square)] \cup \square$ ▷ update set of squares for this cell
    else
      $Y[k(\square)] \leftarrow \{\square\}$ ▷ set of one square
    end if
  end for
  $N \leftarrow 0$
  for each $j \in Y$ such that $Y[j] = X$ **do**
    find boundary $\partial X = \uplus\gamma$ ▷ this is the set of loops γ made of non-shared edges of squares
    for each $\gamma \in \partial X$ **do**
      Let D_j the cell (collection of boxes) with $k(\square) == j$.
      compute the winding number $W(\gamma)$ around loop γ on ∂D_j
      $N \leftarrow N + W(\gamma)$
    end for
  end for
  return $2\pi R^2 N$
end procedure

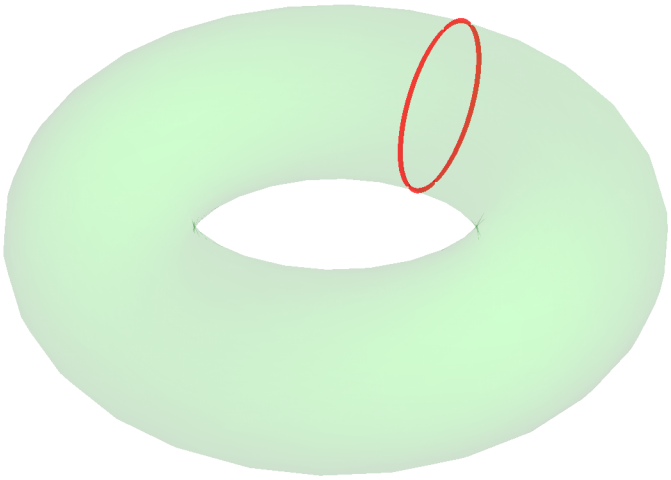

Figure 1: The toroidal vortex cell surrounding the loop C (red).

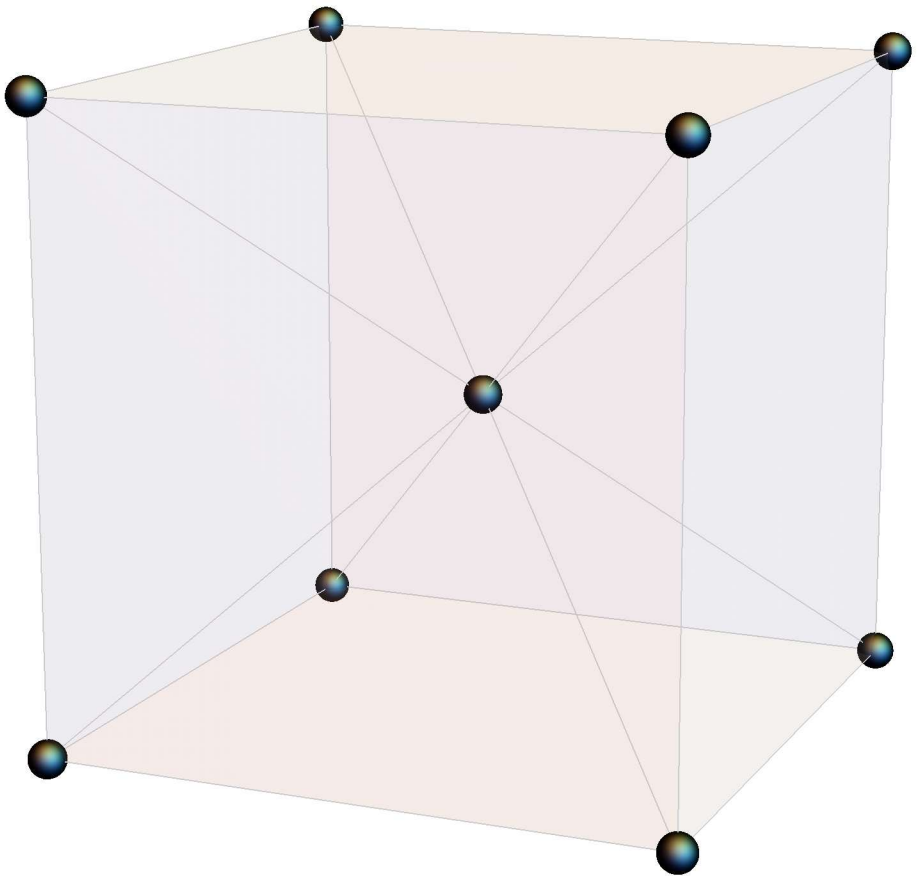

Figure 2: Body Centered Lattice, with the center point associated with Ising spin and 8 vertices - with Clebsch field. Each of 12 edges (links) is associated with kinetic energy term in H_C. There are 4 cubic cells sharing each edge and 8 cells sharing each vertex.

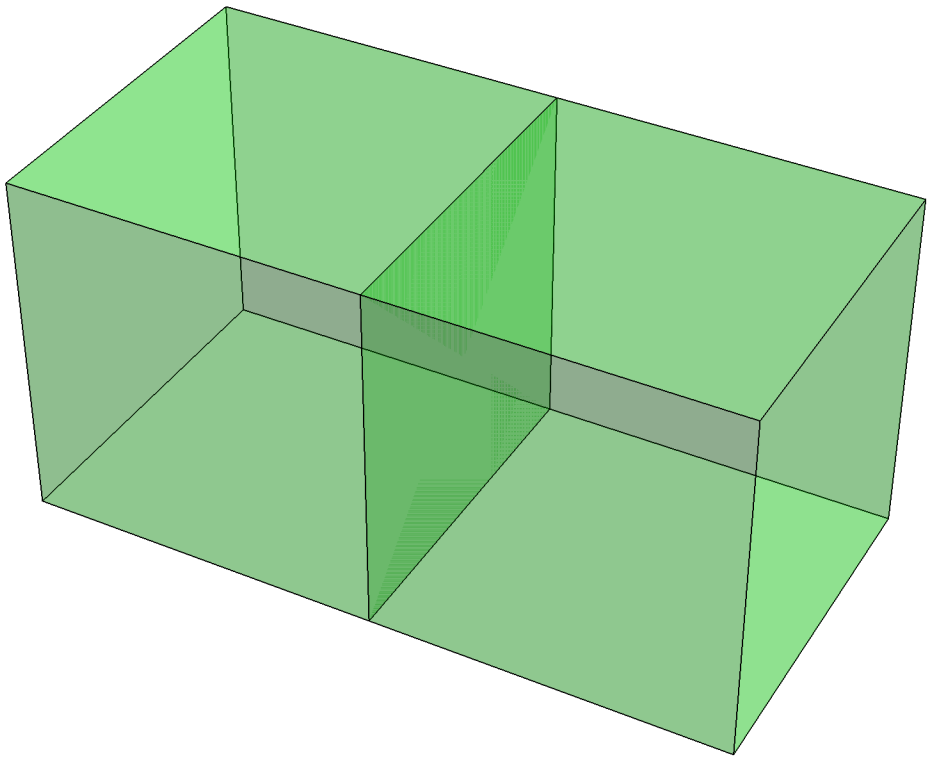

Figure 3: Two cubes touching by a face. These two are neighbors in connectivity graph and the resulting merged cell (common face removed) has Euler characteristic $\chi = 2$ as a sphere.

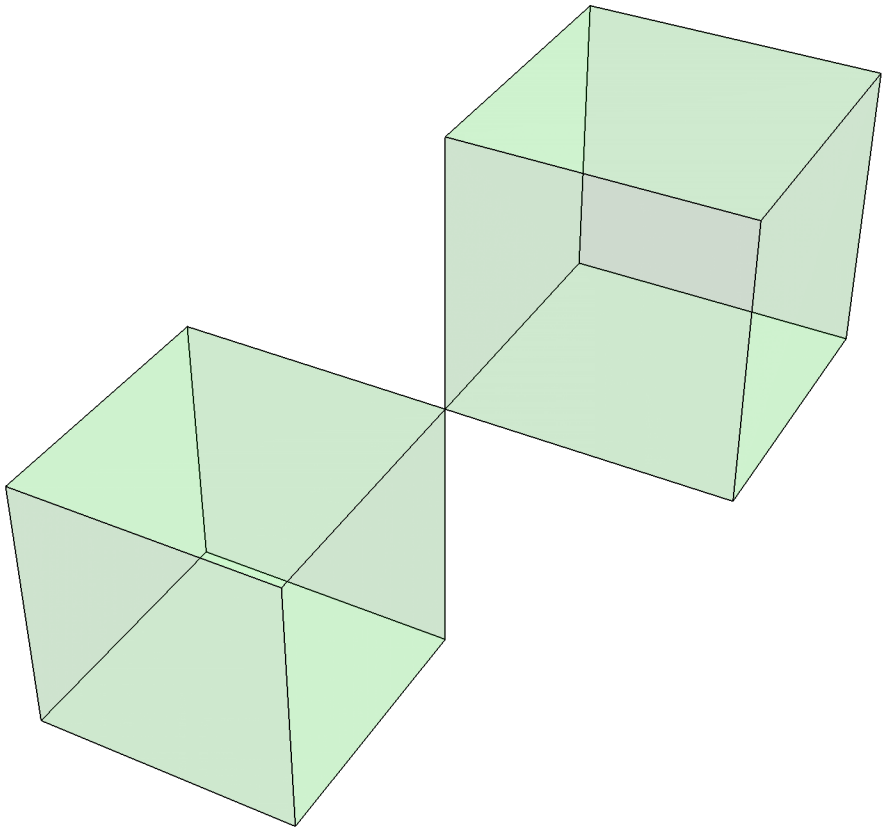

Figure 4: Two cubes touching by a corner. Mathematically, by Euler formula it has $\chi = 3, P = 1$ but for our physics it has $\chi = 4, P = 2$ as two disjoint cubes, because we only count neighbors by face in connectivity graph.

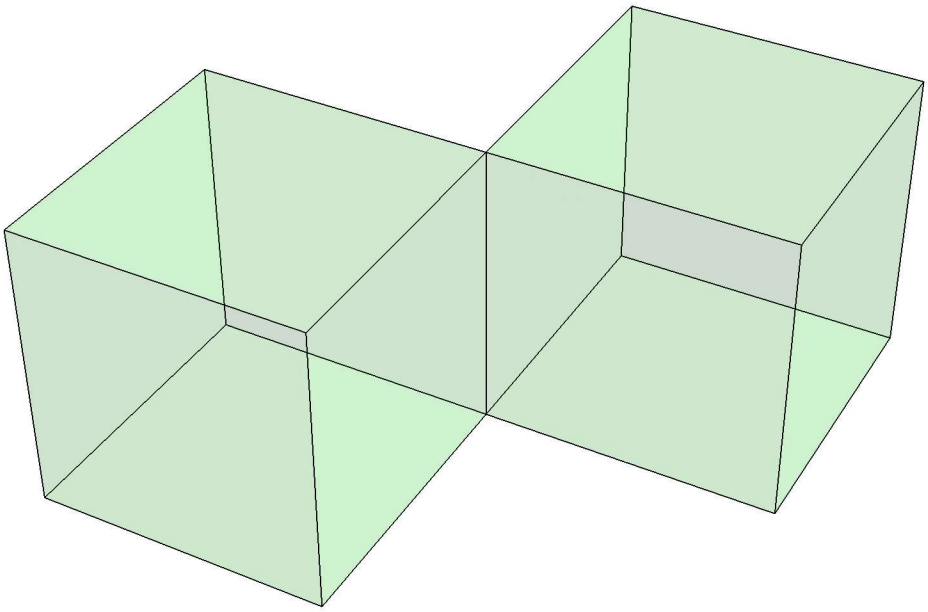

Figure 5: Two cubes touching by an edge.Mathematically, by Euler formula it has $\chi = 3, P = 1$ but for our physics it has $\chi = 4, P = 2$ as two disjoint cubes, because we only count neighbors by face in connectivity graph.

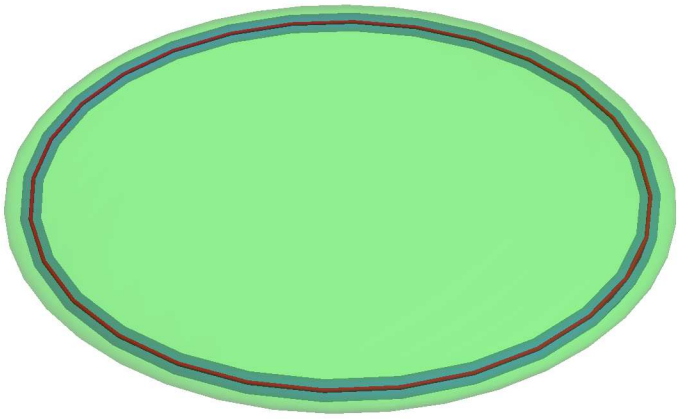

Figure 6: The vortex cell (inside green transparent ellipsoid) with inner wormhole (blue transparent torus) surrounding the loop C (red solid circle).

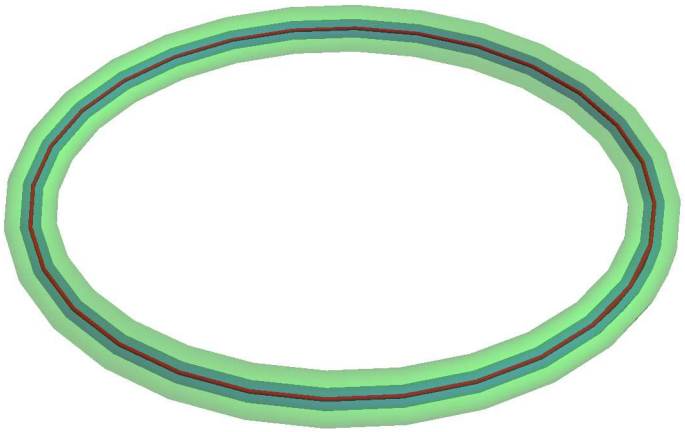

Figure 7: The vortex cell (inside green transparent torus) with inner wormhole (blue transparent torus) surrounding the loop C (red solid circle).

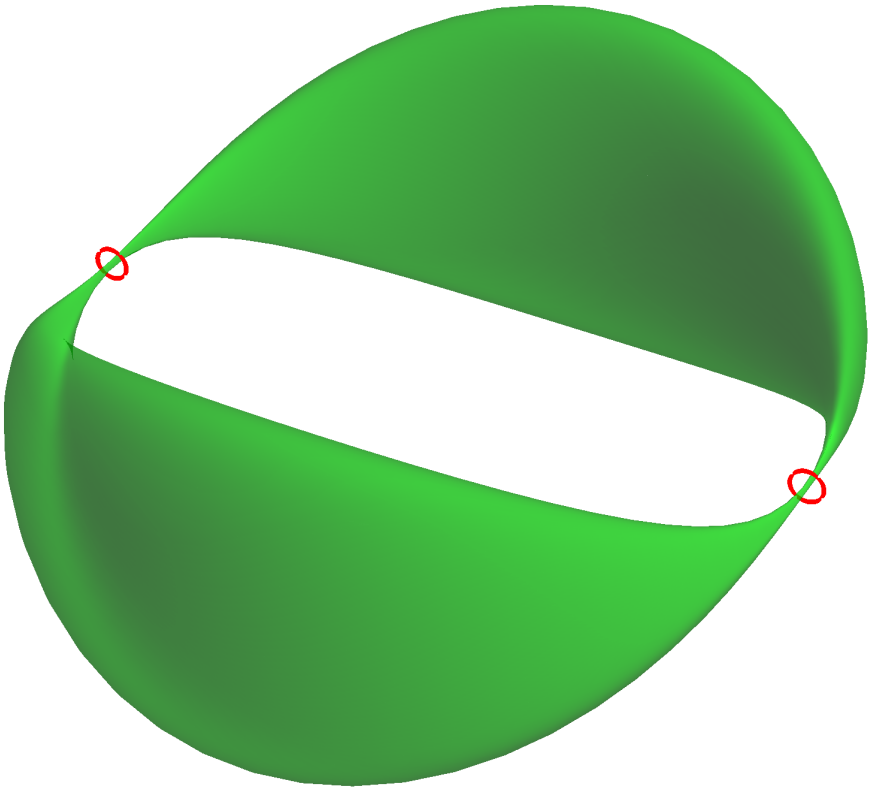

Figure 8: Toroidal vortex cell pinched in two points by loops C_1, C_2, (red circles).

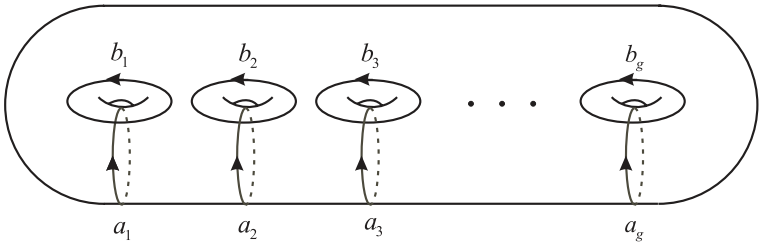

Figure 9: Symplectic Basis on H^1